



Published in final edited form as:

Circ Heart Fail. 2016 January ; 9(1): e002261. doi:10.1161/CIRCHEARTFAILURE.115.002261.

Sympathoexcitation in Rats With Chronic Heart Failure Depends on Homeobox D10 and MicroRNA-7b Inhibiting GABBR1 Translation in Paraventricular Nucleus

Renjun Wang, PhD^{1,2}, Qian Huang, MD³, Rui Zhou, BSc³, Zengxiang Dong, PhD⁴, Yunfeng Qi, PhD¹, Hua Li, MS¹, Xiaowei Wei, MS¹, Hui Wu, MS¹, Huiping Wang, PhD³, Christopher S. Wilcox, MD, PhD⁵, Michael Hultström, MD, PhD^{6,7}, Xiaofu Zhou, PhD¹, and En Yin Lai, MD, PhD^{3,*}

¹ School of Life Science, Jilin Normal University, Siping 136000, China

² Key Laboratory of Cardiovascular Medicine Research of Ministry of Education, Harbin Medical University, Harbin 150086, China

³ Department of Physiology, Zhejiang University School of Medicine, Hangzhou 310058, China

⁴ Department of Cardiology, the First Affiliated Hospital, Harbin Medical University, Harbin 150001, China

⁵ Division of Nephrology and Hypertension, and Hypertension, Kidney and Vascular Health Center, Georgetown University, Washington, DC 20007

⁶ Integrative Physiology, Department of Medical Cell Biology, Uppsala University, Uppsala 75123, Sweden

⁷ Anaesthesia and Intensive Care Medicine, Department of Surgical Sciences, Uppsala University, Uppsala 75123, Sweden.

Abstract

Background—Chronic heart failure (CHF) increases sympathoexcitation through Angiotensin II (ANG II) receptors (AT₁R) in the paraventricular nucleus (PVN). Recent publications indicate down regulation of γ -aminobutyric acid B-type receptor 1 (GABBR1) and has a binding site for microRNA-7b (miR-7b) that is expressed in the PVN. We hypothesized that ANG II regulates sympathoexcitation through homeobox D10 (HoxD10), which regulates miR-7b in other tissues.

Methods and Results—Ligation of the left anterior descendent coronary artery in rats caused CHF and sympathoexcitation. PVN expression of AT₁R, HoxD10 and miR-7b was increased, while GABBR1 was lower in CHF. Infusion of miR-7b in the PVN caused sympathoexcitation in control animals, and enhanced the changes in CHF. Antisense miR-7b infused in PVN normalized GABBR1 expression while attenuating CHF symptoms including sympathoexcitation. A luciferase reporter assay detected miR-7b binding to the 3'-UTR of GABBR1 that was absent after

*Correspondence to: Prof. En Yin Lai, Department of Physiology, Zhejiang University School of Medicine, Hangzhou 310058, China; Tel: +86-571-88208851; Fax: +86-571-88208851, laienyin@zju.edu.cn.

Disclosures
None.

targeted mutagenesis. ANG II induced HoxD10 and miR-7b in NG108 cells, effects blocked by AT₁R-blocker losartan (Los) and by HoxD10 silencing. miR-7b transfection into NG108 cells decreased GABBR1 expression, which was inhibited by miR-7b antisense. *In vivo* PVN knockdown of AT₁R attenuated the symptoms of CHF, while HoxD10 overexpression exaggerated them. Finally, *in vivo* PVN ANG II infusion caused dose dependent sympathoexcitation that was abrogated by miR-7b antisense and exaggerated by GABBR1 silencing.

Conclusions—There is an ANG II/AT₁R/HoxD10/miR-7b/GABBR1 pathway in the PVN that contributes to sympathoexcitation and deterioration of cardiac function in CHF.

Keywords

γ-aminobutyric acid; miR-7b; HoxD10; PVN, ANG II

In chronic heart failure (CHF) increased sympathetic signaling exacerbates cardiac stress, both directly and by stimulating fluid retention by the kidneys through increased renal sympathetic nerve activity (RSNA)¹, which is an important cause of morbidity and mortality^{2, 3}. The paraventricular nucleus (PVN) participates in the regulation of sympathetic outflow⁴⁻⁸. In CHF, ANG II enhances RSNA through stimulation of central AT₁R^{4, 9, 10}, which leads to fluid retention and venous congestion¹¹. ANG II regulates γ-aminobutyric acid (GABA) signaling in the PVN, excites hypothalamic presympathetic neurons¹²⁻¹⁴. GABA-B receptors (GABBR1 and GABBR2) in the PVN are important for the control of sympathetic activity^{15, 16}, but in CHF, their effects are blunted because of GABBR1 gene down-regulation¹⁷. However, the molecular mechanism of decreased GABBR1 gene expression in the PVN during CHF is poorly understood.

MicroRNAs (miRNAs) contribute to regulate gene expression by posttranscriptional binding to the gene 3'-UTR^{18, 19}. miR-7b is highly expressed in the PVN^{20, 21} and its expression is up-regulated after chronic osmotic stress, indicating a role in fluid and electrolyte balance²². However, the role of miR-7b, and that of its regulation by the transcription factor Homeobox D10 (HoxD10)²³ in the PVN during CHF have not been studied. Furthermore, it has been reported that specific miRNAs play an integral role in ANG II receptor (AT₁R) signaling, especially after activation of the Gαq signaling pathway²⁴. We hypothesize that during CHF, ANG II stimulates HoxD10-mediated miR-7b expression in the PVN, in turn contributing to elevated RSNA by inhibiting GABBR1 expression. To test this hypothesis, we infused, in a rat model of CHF, ANG II, adenoviral vectors containing rat AT₁R siRNA (Ad-siAT₁R), adenoviral vectors containing rat HoxD10 (Ad-HoxD10), miR-7b or an inhibitory antisense oligonucleotide, adenoviral vectors containing rat GABBR1 siRNA (Ad-siGABBR1) into the PVN, and we measured cardiac function, haemodynamic parameters, anatomical indications and/or sympathetic drive indicators. Furthermore, *in vivo*, we evaluated AT₁R, HoxD10, miR-7b and GABBR1 expression in the PVN of rats with CHF. In cultured NG108 cells treated with ANG II and the ANG II AT₁R blocker losartan (Los), we determined HoxD10, miR-7b and GABBR1 expression. In cultured HEK293 cells, we determined the binding of miR-7b to the 3'-UTR of GABBR1 gene.

Methods

An expanded methods section is available in the data supplement.

Animals

Male Wistar rats weighing between 180 and 200 grams (Changchun Yisi Laboratory Animal Technology Company, Ltd., Changchun, China) were used to induce CHF by coronary ligation as previously described¹⁷. Catheters were inserted bilaterally into the PVN under anaesthesia using stereotaxic technique²⁵. Drugs were infused using minipumps at doses based on preliminary experiments and previous studies²⁶⁻²⁸. Six weeks after coronary ligation, cardiac function was measured using echocardiography under anaesthesia providing left ventricular diastolic and systolic diameter (LVDD and LVSD), ejection fraction (EF) and fractional shortening (FS)²⁹. In addition, the rats were anaesthetized and prepared for determination of mean arterial blood pressure (MAP), heart rate (HR), left ventricular end diastolic and systolic pressure (LVEDP and LVSP), maximum first differentiation of left ventricle pressure (dp/dtmax), and renal sympathetic nerve activity (RSNA) as described previously²⁶. After the experiment tissue was harvested for further analysis.

Four separate groups of animals were used to study the effect of AT₁R inhibition with Los on the protein expression of HoxD10 and GABBR1, and qPCR for miR-7b (n=6 for each group): sham-operated control (Sham)+vehicle (Veh), Sham+Los, CHF+Veh and CHF+Los. Two weeks after coronary artery ligation Los (10mg/kg/day) was in the drinking water for four weeks before sacrifice. All animals received humane care in compliance with Institutional Animal Care and Use Committees of Jilin Normal University, Zhejiang University, Georgetown University and Uppsala University. Use of animals in this study was confirmed with the Guide for the Care and Use of Laboratory Animals published by the US National Institutes of Health (the 8th Edition).

Gene silencing and transferring in vivo

Recombinant adenoviral vectors (1×10^9 plaque-forming units/ml) harboring rat AT₁R siRNA (Ad-siAT₁R, GenBank accession No. NM74054), rat HoxD10 (Ad-HoxD10, GenBank accession No. NM_001107094), rat GABBR1 siRNA (Ad-siGABBR1, GenBank accession No. NM_031028), or green fluorescent protein siRNA (Ad-siGFP) were manufactured by Vector Gene Technology Company Ltd. (Beijing, China). Corresponding virus with null content (Ad-null) or Ad-siGFP was used as a control. To achieve stable knockdown of AT₁R or GABBR1 in the PVN, we employed adenoviral vectors expressing siRNA targeted against AT₁R or control message (GFP), which were constructed and purified. Briefly, 21 base-pair short hairpin RNA targeting sequences specific for AT₁R, GABBR1 or GFP were engineered under the control of the rat U6 promoter. The hairpin was situated next to the U6 transcription start site (within 6 base pairs) and followed by a synthetic, minimal polyA cassette. PVN infusions were performed 4 weeks prior to subsequent procedures to ensure robust transgene expression.

ANG II infusion

After coronary ligation or sham operation, each rat was anesthetized (60 mg/kg ketamine+5 mg/kg xylazine IP) and underwent subcutaneous implantation of osmotic mini-pumps (Alzet Model #1004). The pumps were connected to bilateral PVN cannulae for continuous infusion (0.11 μ l/h/side) of antagomiR-7b or Ad-siGABBR1 at a total dose of 40 ng/h, NC antagomiR or Ad-siGFP, over a 4-week treatment period. Then the mini-pump (Alzet Model #1004) was replaced by another mini-pump (Alzet Model #1002). Alzet Model #1002 mini-pump were connected to the bilateral PVN cannula for continuous infusion (0.25 μ l/h/side) of ANG II at a total dose of 1 ng/kg per min, over a 2-week treatment period.

Tissue

Plasma was collected for measuring norepinephrine (NE). Heart tissue was used to measure infarction size as previously described¹⁷. Brain sections were stored for histology, and PVN samples were isolated using a micropunch technique^{30, 31}.

In vitro analysis

The concentration of NE in the plasma and ANG II in the PVN was quantified using an ELISA kit (Rocky Mountain Diagnostics, Colorado Spring, Colo), and carried out according to the manufacturer's instructions^{28, 32, 33}. Histological analysis of PVN infusion sites and fluorescence determination of agomiR-7b and antagomiR-7b were performed by standard techniques³⁴. Fra-like (Fra-LI) expression was determined by immunohistochemistry to assess neuronal activation in the PVN³⁵. GABBR1 immunofluorescence was determined by standard techniques using an anti-GABBR1 antibody (Novus Biologicals, Littleton). Western blot for the transcription factor HoxD10 was performed on nuclear protein extract as previously described^{36, 37}. RNA was extracted from PVN micro punches or cultured cells as described in the data supplement. Real-time RT-PCR quantification of miR-7b level and western blot analysis for GABBR1 expression were performed by standard techniques (see data supplement).

Synthesis of agomiRs and miRNA inhibitor antagomiRs

The mature miRNA agomiR-7b and its antisense inhibitor antagomiR-7b were synthesized by GenePharma (Shanghai, China).

Mutagenesis

Nucleotide-substitution mutations were carried out using PCR-based methods for the 3'-UTRs of GABBR1 gene. For rat genes: MT 3'-UTR of GABBR1 gene: 5'-336-AUUUCAGCAGCAGGGCAGAAGGU-358-3' and 5'-833-AGCCUUGUCCUGUCUAGAAGGUG-855-3'. All constructs were sequence verified. The underlined nucleotides indicate the bases where mutations were made, and the numbers before and after the sequences indicate the positions in GABBR1 gene.

Cell culture

HEK293 cells³⁸ (American Type Culture Collection, ATCC, Manassas, VA) and NG108 hybrid (neuroblastoma-glioma) cells^{39, 40} (American Type Culture Collection, ATCC,

Manassas, VA) were cultured with standard techniques. The ability of miR-7b to reduce GABBR1 expression was studied using a luciferase reporter activity assay in HEK293 cells. The luciferase assay and transfection procedures in HEK293 cells were performed as described previously³⁸.

NG108 cells were used to study the effect of miR-7b on GABBR1 by using doses of agomiR-7b (50 nM) and/or antagomiR-7b (100 nM) before western blot. In separate experiments, western blot for GABBR1 was done in control cells, and cells treated with either NC-agomiR-7b (50 nM), agomiR-7b (50 nM), or agomiR-7b (50 nM) and antagomiR-7b (100 nM) in combination. Further, NG108 cells were treated with ANG II (100 μ M)³⁹ or the combination of ANG II (100 μ M) and Los (1 μ M) to study the direct effects on HoxD10 and GABBR1 protein expression with western blot, as well as real-time PCR quantification of miR-7b.

Finally, the role of HoxD10 in the regulation expression of miR-7b and GABBR1 was studied using siRNA knock down in NG108 cells after treatment with ANG II (100 μ M) and the combination of ANG II (100 μ M) and Los (1 μ M). siRNA targeting HoxD10 and its negative control were purchased from from Santa Cruze Inc. (CA, USA).

Data analysis

Group data are expressed as mean \pm SEM. Group differences in the data was tested using two-way ANOVA followed by comparison for individual group differences using the Tukey's test, or one-way ANOVA followed by Dunnett's test where appropriate. The statistical model for the two-way ANOVA used Sham and CHF as one dimension, and treatment groups as the other, or ANG II and Los as dimensions in those experiments. Statistical significance was indicated by $P < 0.05$. All analyses were performed using GraphPad Prism 5.0.

Results

Development of heart failure

Coronary artery ligation caused an average infarct area of $37.4 \pm 2.1\%$ (Table S1) and 90 % of infarcts were transmural, while no infarcts were identified in Sham. Pleural fluid and ascites were found in CHF but not in Sham. CHF as evidenced by an increase in LVDD and LVSD ($P < 0.05$), and reduced EF and FS (Table S1 and S2). CHF rats had increased LVEDP, the right ventricle (RV)/body weight (BW) and lung/BW ratio, while LVSP and $\pm dP/dt_{max}$ were significantly decreased ($P < 0.05$). Heart weight was higher in CHF than in Sham. MAP and HR were not affected by either CHF or Veh infusion into the PVN (Table S3). CHF rats had higher RSNA, and plasma norepinephrine (Figure 1A and 1E), which correlated with a higher PVN Fra-LI activity than untreated Sham (Figure 2A and 2B).

MiRNA treatment *in vivo*

Infusion of agomiR-7b into the PVN produced CHF-like changes with increased left ventricular diameters and reduced EF and FS ($P < 0.05$), and exacerbated the changes seen in CHF. In addition, both Sham and CHF had higher LVEDP, RV/BW and lung/BW ratio

($P < 0.05$), while LVSP and $\pm dP/dt_{max}$ were significantly decreased after agomiR-7b compared to artificial cerebrospinal fluid (aCSF) treated Sham and CHF ($P < 0.05$). The cardiac effects of agomiR-7b were more pronounced in CHF (Table S4 and S5). Further, agomiR-7b increased the sympathetic drive indicators MAP, HR, and RSNA (Figure 1A-1D and 1F) as well as Fra-LI activity (Figure 2A and 2B) in both Sham and CHF. As with the cardiac function and anatomical indicator changes were more pronounced in CHF.

MiRNA inhibition *in vivo*

AntagomiR-7b attenuated the increase in left ventricle dimension and the deterioration of left ventricular performance as indicated by increased EF and FS (Table S2), and improved cardiac function by decreasing LVEDP, increasing LVSP, $+dP/dt_{max}$ and $-dP/dt_{max}$ in CHF animals as well as in agomiR-7b treated Sham and CHF ($P < 0.05$) (Table S4). AntagomiR-7b improved RV/BW and lung/BW ratios in both CHF and agomiR-7b treated Sham and CHF animals (Table S5). Neither aCSF, nor NC agomiR-7b affected echocardiographic or haemodynamic parameters in CHF or Sham (Table S2, S4 and S5).

AntagomiR-7b was able to reduce MAP, HR, and RSNA in both Sham and CHF. As with agomiR-7b the responses were stronger in CHF (Figure 1A-1D and 1F). Further, the increase in plasma NE in CHF could be inhibited with PVN antagomiR-7b (Figure 1E), and Fra-LI activity in the PVN could be reduced (Figure 2A and 2B). Subcutaneous administration of antagomiR-7b did not affect sympathetic signaling as indicated by RSNA, plasma NE, or Fra-LI activity in the PVN (data not shown).

Identification of infusion sites of fluorescence-labelled FAM agomiR-7b and/or antagomiR-7b

Histological analysis showed that agomiR-7b and/or antagomiR-7b-positive cells were localized in the parvicellular and magnocellular divisions of the PVN (Figure S1A). No obvious agomiR-7b and/or antagomiR-7b-positive cell was found in the adjacent brain regions or other areas throughout the brain in most of the rats (Figure S1B).

Molecular regulation of GABBR1 by miR-7b *in vivo*

miR-7b was significantly up-regulated in PVN of CHF compared with Sham rats (Figure 3A). miR-7b can bind to the GABBR1 gene 3'-UTR based on computational and bioinformatics analysis using TargetScan (Wellcome Trust Sanger Institute) (Figure 3B).

Western blot revealed down-regulation of GABBR1 in PVN of CHF when compared to Sham rats ($P < 0.05$, Figure 3C). There was no change in the supraoptic nucleus (Figure 3C). When the luciferase vector carrying the 3'-UTR of GABBR1 was co-transfected with agomiR-7b or ANG II respectively, luciferase activity was robustly diminished compared with transfection of a scrambled miRNA or Veh. The inhibitory effect of agomiR-7b was antagonized by its antisense antagomiR-7b. On the other hand, agomiR-7b did not suppress translation of luciferase transcripts containing the mutant GABBR1 gene 3'UTR (Figure 3D). Further, western blot showed lower GABBR1 levels in the PVN of CHF rats (Figure 4A) and transfection of agomiR-7b in the NG108 cells respectively (Figure 4B), and infusion *in vivo* or transfection *in vitro* of antagomiR-7b prevented this decrease *in vivo*

(Figure 4A) or in vitro (Figure 4B) respectively. Immunofluorescence showed that CHF rats had fewer GABBR1 positive neurons in the PVN than Sham (Figure 4C and 4D). The reduction was exacerbated by agomiR-7b, and alleviated by antagomiR-7b. However, GABBR1 mRNA levels were unchanged by agomiR-7b in both CHF and Sham (Figure S2A).

The role of PVN ANG II *in vivo*

PVN ANG II levels in CHF rats were significantly higher than in Sham rats ($P < 0.05$) (Figure S3A). Infusion of ANG II (0.1, 1, 10 ng/kg per min for 4 weeks) into the PVN increased RSNA and plasma NE (Figure S3B and S3C). The effect on RSNA and plasma NE was greater at any dose in the CHF+Veh group than Sham+Veh group. Infusion of Los prevented this increase. There were no significant differences at any dose between the Sham +Veh and Sham+Los groups (Figure S3B and S3C).

Knockdown of AT₁R in PVN *in vivo*

To investigate the cardiovascular consequences of myocardial infarction (MI)-induced AT₁R upregulation in PVN, we measured the effects of PVN-targeted Ad-siAT₁R on echocardiographic and LV hemodynamic end points in rat 6 weeks after MI or sham surgery. High-resolution ultrasonographic analysis demonstrated normal cardiac function in Sham+Ad-siGFP animals as evidenced by unaltered EF and FS compared to Sham+Ad-siAT₁R (Table S6). In contrast, a marked decrease in EF and FS was observed in rats that underwent MI surgery (Table S6). Importantly, Ad-siAT₁R microinfused into PVN led to significant improvement in lung/BW, RV/BW, LVDd, LVSD, LVEDP, dp/dt, EF, FS and basal RSNA in MI-treated animals, whereas the Sham+Ad-siGFP did not alter either parameter (Table S6).

HoxD10 gene transfer *in vivo*

Compared with Sham-null rats, the lung/BW, RV/BW, LVDd, LVSD, LVEDP and basal RSNA increased, while the dp/dt, FS and EF decreased in CHF-null rats. These changes caused by the MI were significantly enhanced by Ad-HoxD10 (Table S7).

ANG II-induced sympathoexcitation is rescued by antagomiR-7b

Rats treated with PVN ANG II+NC antagomiR-7b had increased HR, MAP, RSNA and plasma NE compared with those of rats treated with PVN NC antagomiR-7b (Table S8). Bilateral PVN infusion of antagomiR-7b prevented the increases in HR, MAP, RSNA and plasma NE observed in ANG II+NC antagomiR-7b treated rats (Table S8).

ANG II-induced sympathoexcitation is enhanced by silencing of GABBR1

Rats treated with PVN ANG II+Ad-siGFP had increased HR, MAP, RSNA and plasma NE compared with those of rats treated with PVN Ad-siGFP (Table S9). Bilateral PVN infusion of Ad-siGABBR1 enhanced, the increases in HR, MAP, RSNA and plasma NE observed in ANG II+Ad-siGFP treated rats (Table S9).

Effects of *in vivo* knockdown silencing of AT₁R in the PVN on HoxD10, GABBR1 protein expression and miR-7b mRNA expression

AT₁R protein expression in the PVN was increased in CHF+Ad-null rats, and reduced by silencing AT₁R (Figure S4A). HoxD10 protein expression in the PVN was increased in CHF+Ad-null rats, and repressed by silencing of AT₁R (Figure S4B). This was associated with similar changes in miR-7b (Figure S4D). However, GABBR1 protein expression in the PVN was decreased in CHF+Ad-null rats, and interestingly rescued by silencing of AT₁R (Figure S4C).

Role of HoxD10 in miR-7b regulation and GABBR1 expression *in vivo*

HoxD10 protein expression in the PVN was increased in CHF rats, and normalized by Los treatment (Figure 5A). This was associated with similar changes in miR-7b (Figure 5C) and a decrease in GABBR1 (Figure 5B). HoxD10 protein expression in the PVN was increased in CHF+Ad-null rats, and enhanced by gene transferring of HoxD10 (Figure S5A). This was associated with similar changes in miR-7b (Figure S5C) and a decrease in GABBR1 (Figure S5B).

Molecular regulation of GABBR1 by miR-7b and HoxD10 *in vitro*

Transfection of agomiR-7b reduced the protein expression of GABBR1 in the PVN (Figure 4A) and in cultured NG108 cells (Figure 4B). This effect was abolished by co-transfection of antagomiR-7b (Figure 4A and 4B). AgomiR-7b did not affect GABBR1 mRNA levels in NG108 cells (Figure S2B). ANG II (100 μM) increased the expression of HoxD10 protein and miR-7b mRNA expression (Figure 6A and 6C), decreased the expression of GABBR1 protein in NG108 cells (Figure 6B), and pretreatment with Los or silencing of HoxD10 using siRNA (HoxD10 siRNA, siHoxD10) ameliorated the effect in NG108 cells (Figure 6A-6C), but the siHoxD10 negative control oligonucleotides did not (data not shown).

ANG II-induced downregulation of GABBR1 is rescued by antagomir-7b

Infusion of ANG II into the PVN downregulated GABBR1 expression (Figure 7). Infusion of antagomiR-7b prevented this downregulation. There were no significant differences between NC antagomiR-7b and antagomiR-7b groups (Figure 7).

Discussion

The main finding in this study was the demonstration of an ANG II/AT₁R/HoxD10/miR-7b/GABBR1 signaling pathway, localized to the PVN, regulating sympathoexcitation, and playing a pathogenic role in CHF. Thereby the present study provides a molecular mechanism for the well-known effect of ANG II on sympathoexcitation in the hypothalamus.

The present result that long-term RSNA is regulated through protein expression effects of microRNA that is stimulated by a specific transcription factor activation by ANG II stimulation of AT₁R in the PVN is important, since sympathetic nerves directly innervate the distal renal tubule and have a significant influence on sodium balance⁴¹. Increased renal sympathetic nerve stimulation is a major mechanism for salt and water retention in patients

with circulatory failure^{1, 41, 42}. Fluid retention in CHF, while necessary to increase preload and maintain cardiac output, leads to venous congestion and potentially decompensation^{1, 43}. Our observations demonstrate that the activity of ANG II and AT₁R in the PVN may play a substantial role in the sympathetic stimulation associated with CHF.

We found that CHF increased the expression of HoxD10 protein and miR-7b, while the expression of GABBR1 protein was decreased in the PVN. In turn, there were larger effects of infusion of both sense and anti-sense miR-7b in rats with CHF, when compared to Sham. These findings indicate that the ANG II/AT₁R/HoxD10/miR-7b/GABBR1 signaling cascade plays an important role in the stimulation of the sympathetic system characteristic of heart failure.

The *in vivo* findings were reproduced in NG108 cells where an enhanced expression of HoxD10 was found after ANG II treatment. A change that could be inhibited by Los or by transfection with a HoxD10 silencer. These results support our findings of miR-7b inhibition of GABBR1 translation in the PVN, an important mechanism for ANG II-induced sympathoexcitation, and confirm that this effect is controlled by HoxD10.

Direct AT₁R stimulation increased HoxD10 and miR-7b expression in the PVN, and decreased GABBR1 expression. The finding that these changes are prevented by AT₁R blockade. Furthermore, AT₁R silencing with using siRNA inhibited the CHF-induced increase of HoxD10 and miR-7b, at the same time, rescued the CHF-induced decrease of GABBR1. This is a novel finding that increasing our understanding of the molecular mechanisms driving enhanced sympathetic activity during CHF.

The effect of HoxD10 on the miR-7 promoter and miR-7 expression has been previously reported²³. The present data reveals, for the first time, that binding of HoxD10 to the miR-7b promoter is important for the ANG II-mediated miR-7b activation in the central nervous system and the PVN. This finding is supported by our observations that transfection with HoxD10 silencer in ANG II-treated NG108 cells reversed the up-regulation of miR-7b nearly back to the control level.

The discovery of HoxD10 and miR-7b expression in the PVN, and their regulation by AT₁R activation during CHF are new findings of importance in cardiovascular physiology and for the pathophysiology of CHF. Further, the expression of miR-7b in PVN and its important role in the regulation of sympathoexcitation through the regulation of GABBR1 translation is an important new finding that improves our understanding of how excessive AT₁R stimulation may drive long-time effects on sympathetic signaling.

The specificity of the present results was demonstrated using infusions of scrambled miRNA, and by peripheral administration of both agonist and antagonist oligonucleotides. Interestingly, the effect of miR-7b on GABBR1 appears to be primarily on the translational level as indicated by changes in GABBR1 protein expression with little effect on mRNA levels, *in vivo* and *in vitro*. These observations suggest that after AT₁R stimulation and during CHF, the GABBR1 protein is downregulated not by mRNA degradation by miR-7b, but by post-transcriptional regulation. The situation is further complicated by the failure of

AT₁R silencing *in vivo* to normalize GABBR1 expression even though it reduced the activation of HoxD10 and miR-7b.

Sympathetic signaling in CHF is known to be differentiated, with marked increased signaling to the kidneys and the heart, while other organs are not as strongly modulated⁴⁴. Although we have strong indications that cardiac and vascular sympathetic nerve activity is regulated by the ANG II/AT₁R/HoxD10/miR-7b/GABBR1 pathway, as measured using HR and MAP, the present data leave unanswered whether the mechanism is important for the differentiation of sympathetic activity between different organs.

In this study CHF was produced by coronary ligation, which is a commonly used model of myocardial infarction. Cardiac function and compensatory hypertrophy is related to time after ligation and infarct area, and were verified in the present project using both cardiac histology, echocardiography and invasive measurement of cardiac function.

In conclusion, in the PVN, ANG II, by AT₁R stimulation enhances sympathetic activity by activating HoxD10, which increases miR-7b expression and thereby reduces GABBR1 translation. ANG II induced HoxD10 activation via a miRNA mediated pathway is a new finding partially clarifying the role of the brain Renin Angiotensin System in cardiovascular regulation. These observations open an interesting area for further study.

Supplementary Material

Refer to Web version on PubMed Central for supplementary material.

Acknowledgements

We thank Prof. Juan M. Saavedra of Georgetown University for helpful comments, language correction and editing during preparation for this manuscript.

Sources of Funding

This study was supported by research grants to E.Y. L., Q. H. and H. W. from the National Nature Science Foundation of China (31471100) and Zhejiang Province Natural Science Foundation (LY13H070002), to R.W. from the National Nature Science Foundation of China (81202527), Program for the Development of Science and Technology of Jilin Province (20130522002JH), the Science and Technology Research Project of Jilin Provincial Department of Education (2015212) and Key Laboratory of Cardiovascular Medicine Research of Ministry of Education, Harbin Medical University (2013001), to Z. D. from Heilongjiang Provincial Government (LBH-Z13160), and to C.S.W. from The National Institute of Diabetes and Digestive and Kidney Diseases (DK-49870 and DK-36079) and The National Heart, Lung, and Blood Institute (HL-68686).

References

1. Jonsson S, Agic MB, Narfstrom F, Melville JM, Hultstrom M. Renal neurohormonal regulation in heart failure decompensation. *Am J Physiol Regul Integr Comp Physiol.* 2014; 307:R493–R497. [PubMed: 24920735]
2. Cohn JN, Levine TB, Olivari MT, Garberg V, Lura D, Francis GS, Simon AB, Rector T. Plasma norepinephrine as a guide to prognosis in patients with chronic congestive heart failure. *N Engl J Med.* 1984; 311:819–823. [PubMed: 6382011]
3. Ferguson DW, Berg WJ, Sanders JS. Clinical and hemodynamic correlates of sympathetic nerve activity in normal humans and patients with heart failure: Evidence from direct microneurographic recordings. *J Am Coll Cardiol.* 1990; 16:1125–1134. [PubMed: 2229759]

4. Liu Q, Wang T, Yu H, Liu B, Jia R. Interaction between interleukin-1 beta and angiotensin ii receptor 1 in hypothalamic paraventricular nucleus contributes to progression of heart failure. *J Interferon Cytokine Res.* 2014; 34:870–875. [PubMed: 24955935]
5. Pyner S. The paraventricular nucleus and heart failure. *Exp Physiol.* 2014; 99:332–339. [PubMed: 24317407]
6. Gan XB, Sun HJ, Chen D, Zhang LL, Zhou H, Chen LY, Zhou YB. Intermedin in the paraventricular nucleus attenuates cardiac sympathetic afferent reflex in chronic heart failure rats. *PLoS One.* 2014; 9:e94234. [PubMed: 24709972]
7. Ruchaya PJ, Antunes VR, Paton JF, Murphy D, Yao ST. The cardiovascular actions of fractalkine/cx3cl1 in the hypothalamic paraventricular nucleus are attenuated in rats with heart failure. *Exp Physiol.* 2014; 99:111–122. [PubMed: 24036597]
8. Ramchandra R, Hood SG, Frithiof R, McKinley MJ, May CN. The role of the paraventricular nucleus of the hypothalamus in the regulation of cardiac and renal sympathetic nerve activity in conscious normal and heart failure sheep. *J Physiol.* 2013; 591:93–107. [PubMed: 22615431]
9. Zhu GQ, Gao L, Patel KP, Zucker IH, Wang W. ANG II in the paraventricular nucleus potentiates the cardiac sympathetic afferent reflex in rats with heart failure. *J Appl Physiol (1985).* 2004; 97:1746–1754. [PubMed: 15475555]
10. Yu XJ, Suo YP, Qi J, Yang Q, Li HH, Zhang DM, Yi QY, Zhang J, Zhu GQ, Zhu Z, Kang YM. Interaction between at1 receptor and nf-kappab in hypothalamic paraventricular nucleus contributes to oxidative stress and sympathoexcitation by modulating neurotransmitters in heart failure. *Cardiovasc Toxicol.* 2013; 13:381–390. [PubMed: 23877628]
11. Stead EA. Renal factor in congestive heart failure. *Circulation.* 1951; 3:294–299. [PubMed: 14812659]
12. Chen Q, Pan HL. Signaling mechanisms of angiotensin ii-induced attenuation of gabaergic input to hypothalamic presympathetic neurons. *J Neurophysiol.* 2007; 97:3279–3287. [PubMed: 17287434]
13. Li DP, Pan HL. Angiotensin ii attenuates synaptic gaba release and excites paraventricular-rostral ventrolateral medulla output neurons. *J Pharmacol Exp Ther.* 2005; 313:1035–1045. [PubMed: 15681656]
14. Chen QH, Toney GM. Responses to gaba-a receptor blockade in the hypothalamic pvn are attenuated by local at1 receptor antagonism. *Am J Physiol Regul Integr Comp Physiol.* 2003; 285:R1231–R1239. [PubMed: 12881200]
15. Li DP, Chen SR, Pan YZ, Levey AI, Pan HL. Role of presynaptic muscarinic and gaba(b) receptors in spinal glutamate release and cholinergic analgesia in rats. *J Physiol.* 2002; 543:807–818. [PubMed: 12231640]
16. Li DP, Pan HL. Role of gamma-aminobutyric acid (gaba)a and gabab receptors in paraventricular nucleus in control of sympathetic vasomotor tone in hypertension. *J Pharmacol Exp Ther.* 2007; 320:615–626. [PubMed: 17071818]
17. Wang RJ, Zeng QH, Wang WZ, Wang W. Gaba(a) and gaba(b) receptor-mediated inhibition of sympathetic outflow in the paraventricular nucleus is blunted in chronic heart failure. *Clin Exp Pharmacol Physiol.* 2009; 36:516–522. [PubMed: 19673934]
18. Xie X, Lu J, Kulbokas EJ, Golub TR, Mootha V, Lindblad-Toh K, Lander ES, Kellis M. Systematic discovery of regulatory motifs in human promoters and 3' utrs by comparison of several mammals. *Nature.* 2005; 434:338–345. [PubMed: 15735639]
19. Jackson RJ, Standart N. How do micrnas regulate gene expression? *Sci STKE.* 2007; 2007:re1. [PubMed: 17200520]
20. Amar L, Benoit C, Beaumont G, Vacher CM, Crepin D, Taouis M, Baroin-Tourancheau A. Microrna expression profiling of hypothalamic arcuate and paraventricular nuclei from single rats using illumina sequencing technology. *J Neurosci Methods.* 2012; 209:134–143. [PubMed: 22687940]
21. Choi JW, Kang SM, Lee Y, Hong SH, Sanek NA, Young WS, Lee HJ. Microrna profiling in the mouse hypothalamus reveals oxytocin-regulating microrna. *J Neurochem.* 2013; 126:331–337. [PubMed: 23682839]

22. Lee HJ, Palkovits M, Young WS. Mir-7b, a microRNA up-regulated in the hypothalamus after chronic hyperosmolar stimulation, inhibits fos translation. *Proc Natl Acad Sci U S A*. 2006; 103:15669–15674. [PubMed: 17028171]
23. Reddy SD, Ohshiro K, Rayala SK, Kumar R. MicroRNA-7, a homeobox d10 target, inhibits p21-activated kinase 1 and regulates its functions. *Cancer Res*. 2008; 68:8195–8200. [PubMed: 18922890]
24. Eskildsen TV, Jeppesen PL, Schneider M, Nossent AY, Sandberg MB, Hansen PB, Jensen CH, Hansen ML, Marcussen N, Rasmussen LM, Bie P, Andersen DC, Sheikh SP. Angiotensin ii regulates microRNA-132/-212 in hypertensive rats and humans. *Int J Mol Sci*. 2013; 14:11190–11207. [PubMed: 23712358]
25. Francis J, MohanKumar SM, MohanKumar PS. Correlations of norepinephrine release in the paraventricular nucleus with plasma corticosterone and leptin after systemic lipopolysaccharide: Blockade by soluble il-1 receptor. *Brain Res*. 2000; 867:180–187. [PubMed: 10837812]
26. Kang YM, Gao F, Li HH, Cardinale JP, Elks C, Zang WJ, Yu XJ, Xu YY, Qi J, Yang Q, Francis J. Nf-kappab in the paraventricular nucleus modulates neurotransmitters and contributes to sympathoexcitation in heart failure. *Basic Res Cardiol*. 2011; 106:1087–1097. [PubMed: 21892747]
27. Kang YM, Wang Y, Yang LM, Elks C, Cardinale J, Yu XJ, Zhao XF, Zhang J, Zhang LH, Yang ZM, Francis J. Tnf-alpha in hypothalamic paraventricular nucleus contributes to sympathoexcitation in heart failure by modulating at1 receptor and neurotransmitters. *Tohoku J Exp Med*. 2010; 222:251–263. [PubMed: 21135513]
28. Kang YM, Ma Y, Elks C, Zheng JP, Yang ZM, Francis J. Cross-talk between cytokines and renin-angiotensin in hypothalamic paraventricular nucleus in heart failure: Role of nuclear factor-kappab. *Cardiovasc Res*. 2008; 79:671–678. [PubMed: 18469338]
29. Pan Z, Zhao W, Zhang X, Wang B, Wang J, Sun X, Liu X, Feng S, Yang B, Lu Y. Scutellarin alleviates interstitial fibrosis and cardiac dysfunction of infarct rats by inhibiting tgfbeta1 expression and activation of p38-mapk and erk1/2. *Br J Pharmacol*. 2011; 162:688–700. [PubMed: 20942814]
30. Palkovits M. Punch sampling biopsy technique. *Methods Enzymol*. 1983; 103:368–376. [PubMed: 6366460]
31. Kang YM, He RL, Yang LM, Qin DN, Guggilam A, Elks C, Yan N, Guo Z, Francis J. Brain tumour necrosis factor-alpha modulates neurotransmitters in hypothalamic paraventricular nucleus in heart failure. *Cardiovasc Res*. 2009; 83:737–746. [PubMed: 19457890]
32. Kang YM, Zhang ZH, Johnson RF, Yu Y, Beltz T, Johnson AK, Weiss RM, Felder RB. Novel effect of mineralocorticoid receptor antagonism to reduce proinflammatory cytokines and hypothalamic activation in rats with ischemia-induced heart failure. *Circ Res*. 2006; 99:758–766. [PubMed: 16960100]
33. Zheng M, Kang YM, Liu W, Zang WJ, Bao CY, Qin DN. Inhibition of cyclooxygenase-2 reduces hypothalamic excitation in rats with adriamycin-induced heart failure. *PLoS One*. 2012; 7:e48771. [PubMed: 23152801]
34. Fan ZD, Zhang L, Shi Z, Gan XB, Gao XY, Zhu GQ. Artificial microRNA interference targeting at(1a) receptors in paraventricular nucleus attenuates hypertension in rats. *Gene Ther*. 2012; 19:810–817. [PubMed: 21956687]
35. Kang YM, Zhang AQ, Zhao XF, Cardinale JP, Elks C, Cao XM, Zhang ZW, Francis J. Paraventricular nucleus corticotrophin releasing hormone contributes to sympathoexcitation via interaction with neurotransmitters in heart failure. *Basic Res Cardiol*. 2011; 106:473–483. [PubMed: 21287352]
36. Weidenfeld-Baranboim K, Bitton-Worms K, Aronheim A. Tre-dependent transcription activation by jdp2-chop10 association. *Nucleic Acids Res*. 2008; 36:3608–3619. [PubMed: 18463134]
37. Schreiber E, Matthias P, Muller MM, Schaffner W. Rapid detection of octamer binding proteins with 'mini-extracts', prepared from a small number of cells. *Nucleic Acids Res*. 1989; 17:6419. [PubMed: 2771659]

38. Yang B, Lin H, Xiao J, Lu Y, Luo X, Li B, Zhang Y, Xu C, Bai Y, Wang H, Chen G, Wang Z. The muscle-specific microRNA mir-1 regulates cardiac arrhythmogenic potential by targeting *gjal* and *kcnj2*. *Nat Med*. 2007; 13:486–491. [PubMed: 17401374]
39. Sharma NM, Llewellyn TL, Zheng H, Patel KP. Angiotensin ii-mediated posttranslational modification of nnos in the pvn of rats with chf: Role for pin. *Am J Physiol Heart Circ Physiol*. 2013; 305:H843–H855. [PubMed: 23832698]
40. Sharma NM, Zheng H, Mehta PP, Li YF, Patel KP. Decreased nnos in the pvn leads to increased sympathoexcitation in chronic heart failure: Role for capon and ANGII. *Cardiovasc Res*. 2011; 92:348–357. [PubMed: 21831995]
41. Koepke JP, DiBona GF. Functions of the renal nerves. *Physiologist*. 1985; 28:47–52. [PubMed: 2858894]
42. Hultstrom M. Neurohormonal interactions on the renal oxygen delivery and consumption in haemorrhagic shock-induced acute kidney injury. *Acta Physiol (Oxf)*. 2013; 209:11–25. [PubMed: 23837642]
43. Zucker IH, Wang W, Brandle M, Schultz HD, Patel KP. Neural regulation of sympathetic nerve activity in heart failure. *Prog Cardiovasc Dis*. 1995; 37:397–414. [PubMed: 7777669]
44. May CN, Frithiof R, Hood SG, McAllen RM, McKinley MJ, Ramchandra R. Specific control of sympathetic nerve activity to the mammalian heart and kidney. *Exp Physiol*. 2010; 95:34–40. [PubMed: 19617268]

CLINICAL PERSPECTIVE

Morbidity and mortality associated with CHF are linked to neurohumoral excitation. Several discrete regions of the central nervous system, such as the PVN, have emerged as primary culprits in driving this neural dysfunction. Although miRNAs within the heart have been implicated in cardiovascular function, it is not known if the function of the miRNA systems in the PVN is altered in the CHF state. The identification of a miRNA mediated pathway in the PVN for cardiovascular regulation opens an interesting area for further study. Inhibition and/or silencing of the ANG II/AT₁R/HoxD10/miR-7b/GABBR1 signaling pathway targeted to the hypothalamus may provide a novel strategy for the treatment of CHF.

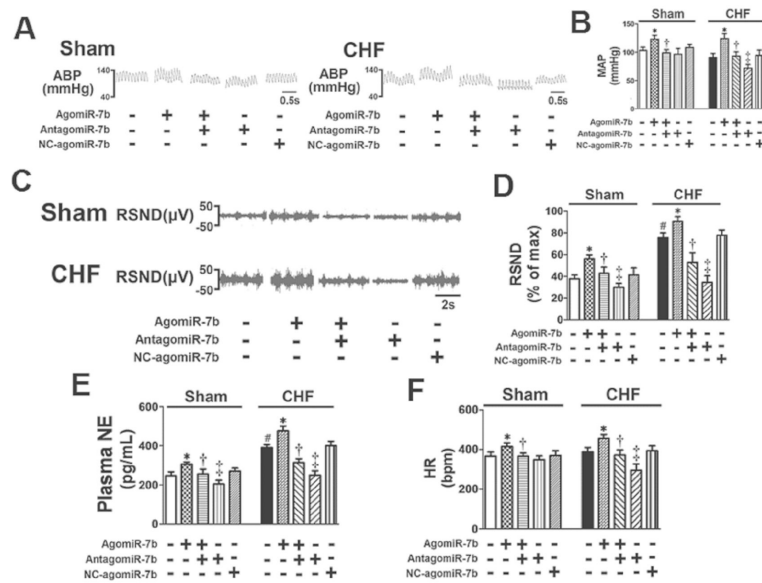


Figure 1. Effects of infusion of agomiR-7b and/or antagonomiR-7b into the PVN on sympathetic drive indicators in Sham and CHF rats

(A) Original tracings of artery blood pressure (ABP). (B) Summarized mean arterial pressure (MAP). Data are expressed as mean±SEM; n=6 for each group; *P<0.05 vs. aCSF or negative control agomiR-7b (NC-agomiR-7b); †P<0.05 vs. agomiR-7b; ‡P<0.05 vs. agomiR-7b+antagonomiR-7b; #P<0.05 Sham+aCSF vs. CHF+aCSF; two-way ANOVA, Tukey test. (C) Original tracings of renal sympathetic nerve activity (RSNA). (D) Summarized RSNA. Data are expressed as mean±SEM; n=6 for each group; *P<0.05 vs. aCSF or negative control agomiR-7b (NC-agomiR-7b); †P<0.05 vs. agomiR-7b; ‡P<0.05 vs. agomiR-7b+antagonomiR-7b; #P<0.05 Sham+aCSF vs. CHF+aCSF; two-way ANOVA, Tukey test. (E) Plasma norepinephrine (NE) concentration. Data are expressed as mean±SEM; n=6 for each group; *P<0.05 vs. aCSF or negative control agomiR-7b (NC-agomiR-7b); †P<0.05 vs. agomiR-7b; ‡P<0.05 vs. agomiR-7b+antagonomiR-7b; #P<0.05 Sham+aCSF vs. CHF+aCSF; two-way ANOVA, Tukey test. (F) Summarized heart rate (HR). Data are expressed as mean±SEM; n=6 for each group; *P<0.05 vs. aCSF or negative control agomiR-7b (NC-agomiR-7b); †P<0.05 vs. agomiR-7b; ‡P<0.05 vs. agomiR-7b+antagonomiR-7b; #P<0.05 Sham+aCSF vs. CHF+aCSF; two-way ANOVA, Tukey test.

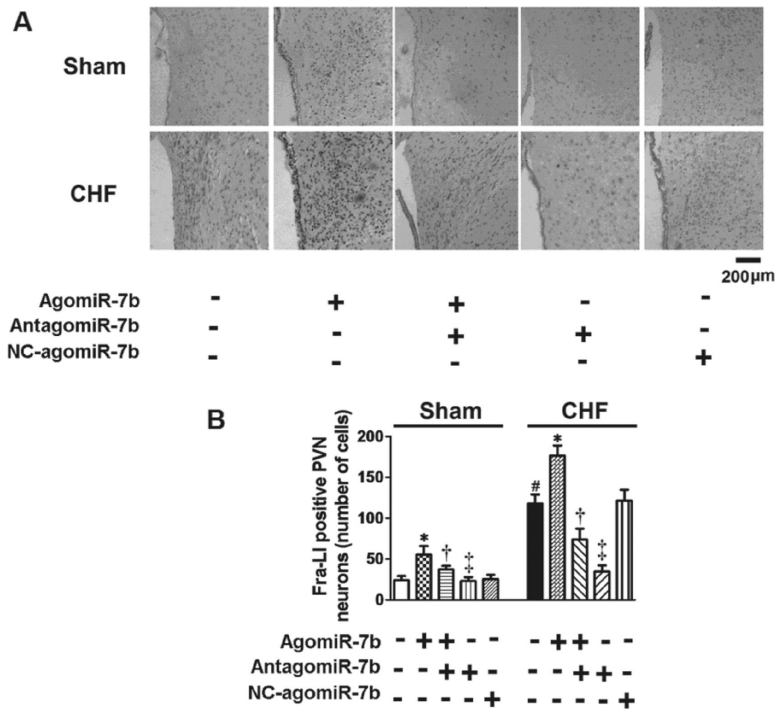


Figure 2. Effects of infusion of agomiR-7b and/or antagomiR-7b into the PVN on numbers of Fra-LI-positive neurons in PVN of Sham and CHF rats

(A) Immunohistochemistry for Fra-LI (black dots) positive neurons in the PVN. Scale bar: 200 μm. (B) Bar graph comparing Fra-LI-positive neurons in the PVN. Data are expressed as mean±SEM; n=6 for each group; *P<0.05 vs. aCSF or NC-agomiR-7b; †P<0.05 vs. agomiR-7b; ‡P<0.05 vs. agomiR-7b+antagomiR-7b; #P<0.05 Sham+aCSF vs. CHF+aCSF; two-way ANOVA, Tukey test.

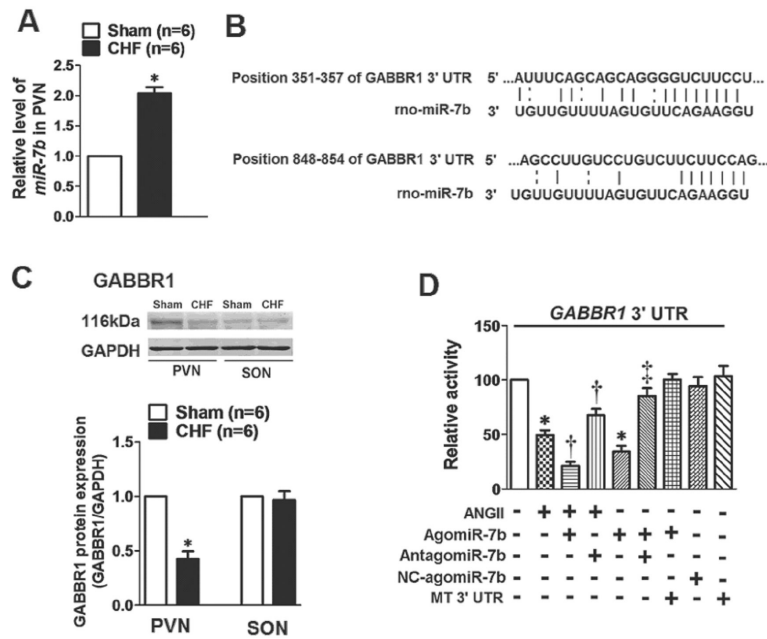


Figure 3. Upregulated miR-7b inhibition of GABBR1 expression in the PVN in CHF rats (A) Relative expression of miR-7b mRNA in PVN of Sham and CHF rats. Data are expressed as mean±SEM normalized to Sham; * $p < 0.05$ vs. Sham; one-way ANOVA, Dunnett *t*-test. (B) Complementary sequences to miR-7b in the 3'UTRs of rat GABBR1 mRNAs. Complementary bases are shown in bold and connected by "I", and matched base "G" and "U" connected by ":". (C) Protein expression of GABBR1 in the PVN and supraoptic nuclei (SON) in Sham and CHF rats. Blots are typical, examples from Sham (□) and CHF (■) rats. Data are expressed as mean±SEM normalized to Sham; $n = 6$ each group; * $P < 0.05$ vs. Sham; one-way ANOVA, Dunnett *t*-test. (D) Verification of interactions among ANG II, rat agomiR-7b and the 3'-UTRs of rat GABBR1 gene in HEK293 cells, determined by luciferase reporter activity. MT 3' UTR, mutant GABBR1 gene 3' UTR. Data are expressed as mean±SEM normalized to aCSF; $n = 6$ each group; * $P < 0.05$ vs. aCSF or NC-agomiR-7b; † $P < 0.05$ vs. ANG II; ‡ $P < 0.05$ vs. agomiR-7b; one-way ANOVA, Dunnett *t*-test.

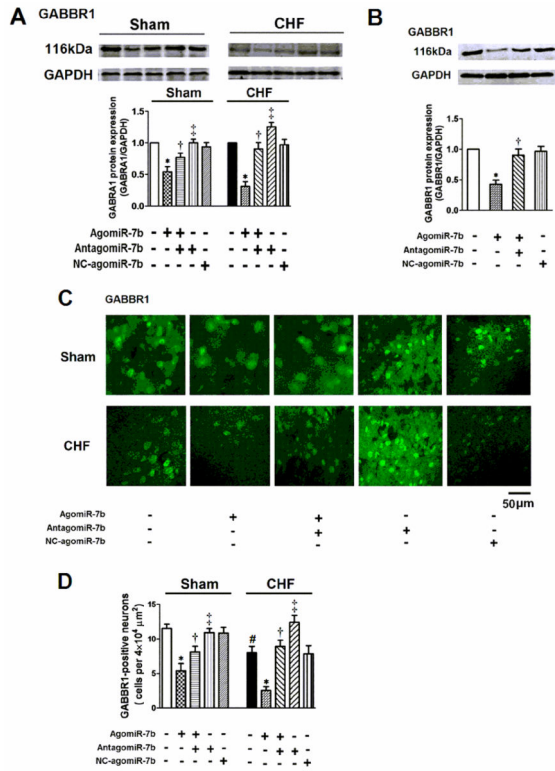


Figure 4. Effects of agomiR-7b and/or antagomiR-7b treatment on GABBR1 protein expression *in vivo* and *in vitro*
(A) Effects of agomiR-7b on expression of GABBR1 protein in the PVN. Data are expressed as mean±SEM normalized to Sham+aCSF or CHF+aCSF; n=6 for each group; *P<0.05 vs. aCSF or NC-agomiR-7b; †P<0.05 vs. agomiR-7b; ‡P<0.05 vs. agomiR-7b +antagomiR-7b; two-way ANOVA, Tukey test. **(B)** Effects of miR-7b on levels of GABBR1 protein in cultured NG108 cells. Data are expressed as mean±SEM normalized to aCSF; n=6 for each group; *P<0.05 vs. aCSF or NC-agomiR-7b; †P<0.05 vs. agomiR-7b; one-way ANOVA, Dunnett *t*-test. **(C)** Immunofluorescent verification of repression of GABBR1 by miR-7b in the PVN. **(D)** Comparison of GABBR1 positive neurons in the PVN. Data are expressed as mean±SEM; n=6 for each group; *P<0.05 vs. aCSF or NC-agomiR-7b; †P<0.05 vs. agomiR-7b; ‡P<0.05 vs. agomiR-7b+antagomiR-7b; #P<0.05 Sham +aCSF vs. CHF+aCSF; two-way ANOVA, Tukey test.

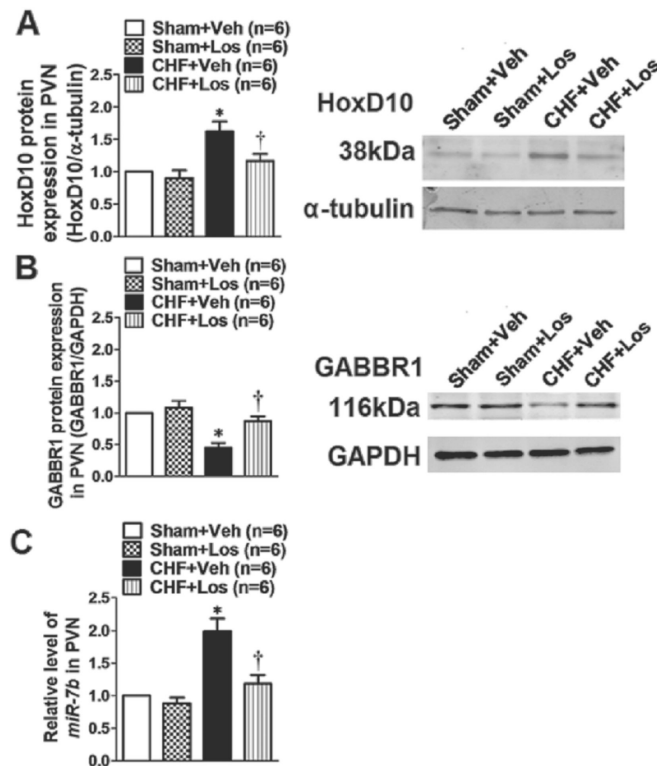


Figure 5. Effects of *in vivo* Los treatment on HoxD10 and GABBR1 protein expression and miR-7b mRNA expression

(A) *In vivo* regulation of HoxD10 protein expression by Los. Right panel, a typical western blot; left panel, data are expressed as mean±SEM normalized to Sham+Veh; *P<0.05 vs. Sham+Veh; †P<0.05 vs. CHF+Veh; two-way ANOVA, Tukey test. (B) *In vivo* regulation of GABBR1 protein expression by Los. Right panel, a typical western blot; left panel, data are expressed as mean±SEM normalized to Sham+Veh; *P<0.05 vs. Sham+Veh; †P<0.05 vs. CHF+Veh; two-way ANOVA, Tukey test. (C) Los suppressed miR-7b mRNA expression. Data are expressed as mean±SEM normalized to Sham+Veh; *P<0.05 vs. Sham+Veh; †P<0.05 vs. CHF+Veh; two-way ANOVA, Tukey test.

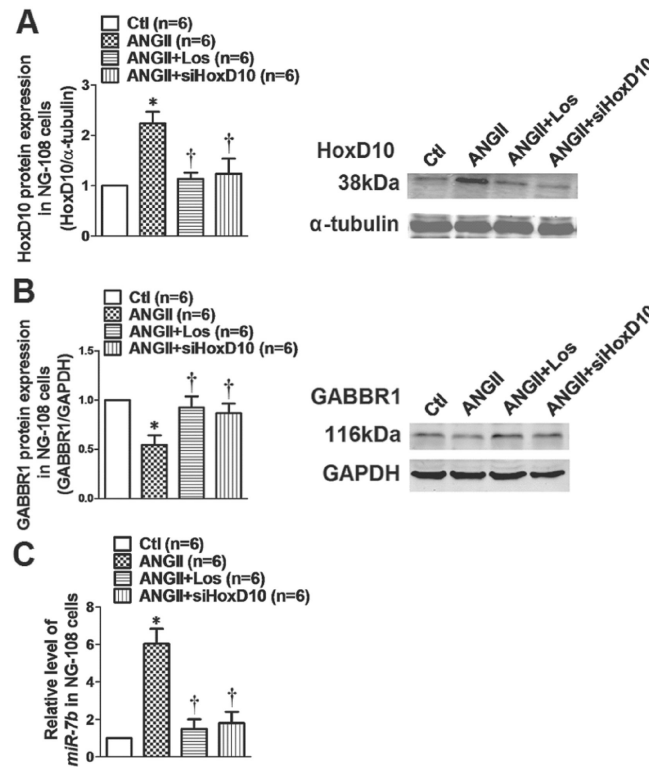


Figure 6. Effects of ANG II, ANG II+Los and ANG II+siHoxD10 on expression of HoxD10, GABBR1 protein and miR-7b mRNA in NG108 cells

(A) *In vitro* regulation of HoxD10 protein expression by ANG II, ANG II+Los and ANG II +siHoxD10. Right panel, pictures of a typical western blot; left panel, quantitative data are expressed as mean±SEM normalized to aCSF; two-way ANOVA, Tukey test. (B) *In vitro* regulation of GABBR1 protein expression by ANG II, ANG II+Los and ANG II+siHoxD10. Right panel, a typical western blot; left panel, quantitative data are expressed as mean±SEM normalized to aCSF; two-way ANOVA, Tukey test. (C) *In vitro* regulation of miR-7b mRNA expression by ANG II, ANG II+Los and ANG II+siHoxD10. Data are expressed as mean±SEM normalized to aCSF; *P<0.05 vs Veh; †P<0.05 vs. ANG II; two-way ANOVA, Tukey test.

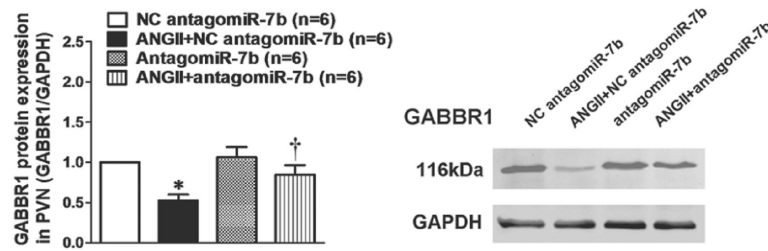


Figure 7. ANG II-induced downregulation of GABBR1 is rescued by antagomiR-7b
In vivo regulation of GABBR1 protein expression by infusion of ANG II and/or antagomiR-7b. Right panel, a typical western blot; left panel, data are expressed as mean \pm SEM normalized to NC antagomiR-7b; * $P < 0.05$ vs. NC antagomiR-7b; † $P < 0.05$ vs. ANG II+NC antagomiR-7b; one-way ANOVA, Dunnett *t*-test.